Medicine®

QUALITY IMPROVEMENT STUDY

OPEN

Assessing Region of Interest Schemes for the Corticospinal Tract in Patients With Brain Tumors

Chen Niu, PhD, Xin Liu, PhD, Yong Yang, PhD, Kun Zhang, PhD, Zhigang Min, MD, Maode Wang, MD, Wenfei Li, MD, Liping Guo, PhD, Pan Lin, PhD, and Ming Zhang, MD

Abstract: Diffusion tensor imaging (DTI) and diffusion tensor tractography (DTT) techniques are widely used for identifying the corticospinal tract (CST) white matter pathways as part of presurgical planning. However, mass effects in patients with brain tumors tend to cause anatomical distortions and compensatory functional reorganization of the cortex, which may lead to inaccurate mapping of white matter tracts. To overcome these problems, we compared different region-of-interest (ROI) selection schemes to track CST fibers in patients with brain tumors. Our study investigated the CSTs of 16 patients with intracranial tumors. The patients were classified into 3 subgroups according to the spatial relationships of the lesion and the primary motor cortex (PMC)/internal capsule. Specifically, we investigated the key factors that cause distorted tractography in patients with tumors. We compared 3 CST tractography methods that used different ROI selection schemes. The results indicate that CST fiber tracking methods based only on anatomical ROIs could possibly lead to distortions near the PMC region and may be unable to effectively localize the PMC. In contrast, the dual ROI method, which uses ROIs that have been selected from both blood oxygen level-dependent functional MRI (BOLD-fMRI) activation and anatomical landmarks, enabled the tracking of fibers to the motor cortex. The results demonstrate that the dual ROI method can localize the entire CST fiber pathway and can accurately describe the spatial relationships of CST fibers relative to the tumor. These results illustrate the reliability of using fMRI-guided DTT in patients with tumors. The combination of fMRI and anatomical information enhances the identification of tracts of interest in brains with anatomical deformations, which provides neurosurgeons with a more accurate approach for visualizing and localizing white matter fiber tracts in patients with brain tumors. This approach enhances surgical performance and perserves brain function.

(*Medicine* 95(12):e3189)

Abbreviations: 3D = three-dimensional, BOLD = blood oxygen level-dependent, CST = corticospinal tract, DTI = diffusion tensor imaging, DTT = diffusion tensor tractography, fMRI = functional magnetic resonance imaging, FWHM = full-width-half-maximum, GLM = general linear model, PMA = primary motor area, ROI = region of interest, WHO = World Health Organization.

INTRODUCTION

For clinical neurosurgery, maximal brain tumor resection and preservation of brain function is critical in improving postoperative outcomes.[1,2] Anatomical distortions and a functional reorganization of the cortex may occur in patients with mass lesions.[3,4] Functional and structural mapping of lesions and the adjacent tissue could reduce the risk of damage to normal tissue in neurosurgery, thus preserving brain function.[5–7]

Blood oxygen level-dependent functional MRI (BOLD-fMRI) is a widely used noninvasive imaging technique for the presurgical localization of eloquent areas, including the sensorimotor cortex, language cortex, and subcortical structures.[8–11] Therefore, presurgical task-based fMRI may provide information on neurological functional for presurgical planning that can help maximize the resection of tumor tissue while preserving eloquent brain areas.[12–14]

The corticospinal tract (CST) is demonstrated to be a major tract for motor control functions. Its integrity is essential for postoperative preservation of motor functions.[15,16] Preservation of the CST is essential for motor function in patients with brain tumors. Negligent transection of CST fibers may cause damage of motor functions.[17] However, BOLD-fMRI and conventional T1-weighted MR structural images cannot provide structural information about the CST for the resection of eloquent motor lesions.

Diffusion tensor imaging (DTI) is a noninvasive magnetic resonance method that provides information on the microstructural organization of white matter in vivo,[18,19] and it is useful for the reconstruction and visualization of white matter tracts.[20,21] Previous studies have shown that CST fiber tracking based on anatomical landmarks could be used to visualize the CST in patients with brain tumors and to delineate the safety margins for surgical planning.[22–24] However, intersubject anatomical variations make it difficult to define tracking seed areas based merely on reliable anatomical landmarks, even in the brains of healthy subjects.[25] In patients with a brain tumor, white matter could deviate from its original location, or anatomical

Editor: Kavindra Nath.
Received: December 1, 2015; revised: February 28, 2016; accepted: March 3, 2016.
From the Department of Medical Imaging, The First Affiliated Hospital of Xi'An Jiaotong University, Xi'an, Shaanxi (CN, MG, WL, LG, MZ); Key Laboratory of Biomedical Information Engineering of Education Ministry, Institute of Biomedical Engineering, Xi'an Jiaotong University, Xi'an (XL); School of Information Technology, Jiangxi University of Finance and Economics, Nanchang, People's Republic of China (YY); Department of Electronics Engineering, Northwestern Polytechnical University, Xi'an (KZ); Department of Neurosurgey, First Affiliated Hospital of Xi'An Jiaotong University, Xi'an, Shaanxi (MW); Key Laboratory of Biomedical Information Engineering of Education Ministry, Institute of Biomedical Engineering, Xi'an Jiaotong University, Xi'an (PL); and Department of Medical Imaging, The First Affiliated Hospital of Xi'An Jiaotong University, Xi'an (MZ), Shaanxi, China.
Correspondence: Pan Lin, PhD, Key Laboratory of Biomedical Information Engineering of Education Ministry, Institute of Biomedical Engineering, Xi'an Jiaotong University, Xi'an 710049, China (e-mail: linpan@mail.xjtu.edu.cn).
Correspondence: Ming Zhang, MD, Department of Medical Imaging, First Affiliated Hospital of Xi'An Jiaotong University College of Medicine, Shaanxi Xi'an 710061, China (e-mail: zmmri@163.com).
CN and XL contributed equally in this article.s
The authors report no conflicts of interest.
Supplemental Digital Content is available for this article.

ISSN: 0025-7974
DOI: 10.1097/MD.0000000000003189

TABLE 1. Demographics Information and Tumor Type

No.	Sex	Age, y	Tumor Location	Tumor Type	Tumor Involve PMC	Tumor Involve Internal Capsule
01	F	49	Left frontal/parietal	Microcystic Meningioma	Y	N
02	F	48	Right frontal	Transitional Meningioma	N	N
03	F	46	Left parietal	Transitional Meningioma	Y	N
04	M	74	Left parietal	Transitional Meningioma	Y	N
05	F	41	Left frontal	Astrocytoma (Grade II)	N	N
06	F	44	Left frontal/parietal	Astrocytoma (GradeII∼III)	Y	N
07	M	55	Right frontal/parietal/temporal	Astrocytoma (Grade III∼IV)	Y	Y
08	M	38	Left frontal	Oligodendroglioma (Grade II)	N	N
09	M	47	Left frontal	Astrocytoma (Grade II)	N	N
10	M	70	Right parietal	Metastatic (squamouscarcinoma)	Y	N
11	M	53	Left frontal/parietal	Astrocytoma (GradeII∼III)	Y	N
12	M	42	Left parietal/occipital	Oligodendroglioma (Grade II)	Y	Y
13	M	63	Right parietal	Anaplastic Astrocytoma	Y	Y
14	M	43	Left frontal/parietal	Astrocytoma (GradeI∼II)	N	N
15	M	51	Left frontal/temporal	Astrocytoma (GradeII∼III)	Y	Y
16	M	67	Left temporal/occipital	Astrocytoma (GradeIII)	Y	Y

PMC = primary motor cortex.

distortions may be present because of the mass effect.[26,27] In such cases, defining fiber tracking ROIs based on anatomical landmarks could be misleading. To overcome this problem, several studies have attempted to integrate fMRI information with DTT to define cortical ROIs. Previous findings have demonstrated that a combination of fMRI and DTT can provide a more comprehensive visualization of the CST in its entirety.[25,28]

Current approaches combining BOLD-fMRI and DTT methods have not been able to overcome problems with tractography in patients with tumors. It is worth noting that the hemodynamic response and neurovascular coupling might be altered in tumor-infiltrated regions,[29–31] which could lead to inaccurate BOLD-fMRI activation results. Furthermore, other clinical problems could arise from the patient being uncooperative during fMRI scanning, which would result in inaccurate BOLD-fMRI activation pattern. In addition, intracranial tumors could cause edema and the destruction or infiltration of white matter fibers, which interfere with the diffusion process, leading to spurious tractography results.[27,32,33] These problems can be partly resolved by adding an additional ROI along the CST pathway. However, the most effective way to use fMRI-guided DTI for CST fiber tracking remains unknown. Our goal is to lower the risk of inaccuracies in fMRI activation patterns and spurious tractography results by combining anatomical landmarks and functional information.

The aim of the present study was to investigate whether a different ROI definition method, such as the integration of BOLD-fMRI and DTI, could improve the accuracy of the evaluation of the spatial relationship between the CST and the borders of the tumor for surgical planning. By dividing patients into subgroups according to the spatial relationship of their lesion and the primary motor area (PMA)/internal capsule, we investigated the primary factors that cause distorted tractography results in patients with tumors. We hypothesized that fMRI-guided DTI tractography with a second subcortical ROI could be used to mitigate the problems caused by an intracranial space-occupying tumor and, therefore provide a more accurate localization of the CST and more accurate data for preoperative decisions.

MATERIALS AND METHODS

Patients

We consecutively evaluated 86 patients with brain tumors using conventional MRI. These patients were registered at the First Affiliated Hospital of Xi'an Jiaotong University between May 2012 and March 2014. We reviewed all conventional MRI scans obtained before surgery and, the postsurgical pathology results. Sixteen patients who were diagnosed with brain tumors were involved in this study (11 men, 5 women; age 38 to 74 years, mean age of 51.93 ± 10.99 years; Table 1). Inclusion criteria were as follows: age >18 years (no upper limit), right-handed, and the presence of a single space-occupying lesion located in one hemisphere (4 were in the right hemisphere and 12 were in the left hemisphere) that was recognized based on a previous computed tomography or MRI examination (with or without contrast medium). Patients with a history of neurological or psychiatric disorders were excluded. All of the patients required neurosurgery for an intracranial lesion. Based on the histological features of the tumor, as determined by biopsy and according to the World Health Organization criteria,[34] 9 cases were identified as astrocytomas, 4 were meningiomas, 1 was a metastatic tumor, and 2 were oligodendrogliomas. Table 1 summarizes all of the patient information. Preoperatively, all of these patients underwent a neuropsychological evaluation, a conventional MRI scan, a functional MRI scan, and a DTT scan. The local institutional ethics committee on human research of the First Affiliated Hospital of Xi'an Jiaotong University approved this study, and the clinical data were acquired following the guidelines of the Department of Neurosurgery. Informed consent was obtained from all of the patients who participated in this study.

Motor Task

The motor task is a block-design sequences (ABABABABABA), consists of 6 rest periods (A) and five hand movement periods (B). Each period lasted 30 seconds, and the total duration of motor task scan was 330 seconds. During the task, the subjects were asked to open and close both hands

repetitively when they saw the flash visual cue display in the mirror. Before the experiment, subjects were trained to perform the motor task outside the scanner to ensure that they understood the task. We presented the motor task stimuli by E-Prime Version 2.0 (Psychology Software Tools, Pittsburgh, PA) through the liquid crystal display projector. The subjects viewed the stimuli through the mirror mounted on top of a head coil.

MRI Data Acquisition

Images were acquired with a 3.0T whole-body MR scanner (GE Signa HDxt, Milwaukee, WI), equipped with an 8-channel head receiver coil. Foam padding and headphones were used to limit head motion and reduce scanner noise.

The functional and structural imaging data were carried out same protocol by our previous study.[14]

Structural images were acquired using a fast-spoiled gradient echo (FSPGR) 3-dimensional T1-weighted sequence (TR = 10.8 ms, TE = 4.8 ms, TI = 1020 ms, flip angle = 15 degree, FOV = 256 mm, matrix size = 256 × 256, slice thickness = 1 mm without gap, voxel size = $1 \times 1 \times 1\ mm^3$). A total of 150 axial slices were acquired to cover the whole brain.

The BOLD-fMRI imaging data were acquired using an echo-planar-imaging (EPI) sequence (TR = 2500 ms; TE = 40 ms; acquisition matrix = 64 × 64; slice thickness = 3 mm; voxel size = $3.75 \times 3.75 \times 3\ mm^3$; FOV = 256 mm). One hundred fifty volumes were acquired as fMRI series.

The parameters used for DTI data acquisition were as follows: TR = 8000 ms, TE = 86 ms, acquisition matrix = 128 × 128, (reconstructed to an image matrix = 256 × 256), voxel size = $0.938 \times 0.938 \times 5\ mm^3$, slice thickness = 5 mm with no gaps, and an acceleration factor for parallel imaging = 2. A total of 28 contiguous slices were acquired for b values of 0 and 1000 s/mm^2 using gradients along 30 different diffusion directions in 4 min and 14 s.

Data Analysis

The analysis for each technique (BOLD-fMRI and DTI) was performed separately. The analysis was performed on data at the single-subject data level because of variability in the clinical cases and the nature and locations of their brain lesions. Figure 1 shows a flow chart of the data processing steps.

BOLD-fMRI Analysis

The BOLD-fMRI dataset was analyzed using toolboxes from FMRIB Software Library (www.fmrib.ox.ac.uk/fsl/). For each subject, the first 4 scans were excluded from analysis to avoid initial unestablished signal. The motion correction was performed using motion correction FLIRT (MCFLIRT). Spatial smoothed with a Gaussian kernel of 6 mm full width at half maximum (FWHM) was applied to the brain images. High-pass filter with cutoff frequency of 0.01 Hz was applied to temporal fMRI signal to remove noise trends with low frequency. The functional images were normalized to the MNI152 standard space using affine transformations. Functional activation statistical analysis was performed for each subject using FSL FEAT tool based on General linear model (GLM). Functional statistical mapping were thresholded at whole brain level using clusters determined by $Z > 2.3$ (corrected cluster threshold $P < 0.05$). The motor activation regions were as follows: left primary motor cortex (PMC), right PMC, and supplementary motor area. The center of each motor activation region was determined by the coordinates of the local z value maxima on functional activation map. The functional ROI was defined as a 6 mm sphere centered at the center of each motor activation region.

DTI Analysis

Diffusion tensor images were processed using the FMRIB's Diffusion Toolbox (FDT 2.0) from the FMRIB's Software Library (FSL, version 4.1.4, http://www.fmrib.ox.ac.uk/fsl).[35–37] The raw DTI data were corrected for eddy currents and head motion, and data relating to non-brain tissue was removed using the brain extraction tool. Diffusion tensor models were then fitted independently for each voxel within the brain. CST probabilistic tractography was performed on each individual's native DTI data. To define the anatomical ROI, the pons ROI (ROI1) was manually defined in the individual subject's color-coded fractional anisotropy (See Figure 1), and then, the anatomical ROI was constructed by forming a 2-mm sphere ROI. To define the fMRI-based functional ROI (ROI2), we defined the PMC motor ROI using the motor task activation maps in the fMRI native space for each individual. Then, the PMC ROI was transformed into the individual subject's DTI image space using linear registration (FLIRT). CST tractography was performed using ROI1, ROI2, and a dual ROI (ROI1 + ROI2) approach. The dual approach uses the fMRI activation of ROI2 as a seed region and the anatomical ROI1 (pons) as a target region. A probabilistic tractography analysis was performed using ProbtrackX in FDT. Tracking was performed in the diffusion space. The probabilistic tractography analysis was performed using 5000 streamline sample fibers within each voxel with a curvature threshold of 0.2, a step length of 0.5, and a maximum number of 2000 steps. At the individual level, the CST tracts were thresholded using 20% of the samples to remove the voxels with a low probability of connection. Finally, the tractography results were then transformed back into the anatomical space using linear registration (FLIRT).

RESULTS

Patients with a Tumor in the PMC that Did Not Affect the Internal Capsule

Group I patients (patients 1, 3, 4, 6, 10, and 11) had a tumor in the PMC that did not affect the internal capsule. Figure 2 shows patient 1's CST fiber tracking results using the 3 different ROI approaches. Patient 1 had a confirmed pathological diagnosis of microcystic meningioma in the left frontoparietal lobe. In this case, the patient's lesion was located in the left PMC and did not affect the left internal capsule. Figure 2A displays the lesion and the motor-activated area on a T1-weighted image. Figure 2B shows the CST fiber tracking results based on different ROIs; yellow, green, and purple represent the CST fiber tracking results obtained by using ROI1, ROI2 and ROI1 + ROI2, respectively. Figure 2C shows the 3D visualization of the CST fiber tracking results based on different ROI definitions. These results indicate that the lesion in the left frontoparietal lobe had a significant mass effect on the CST. We were able to successfully track fiber related to hand movement when using the fMR I-based definition of the ROI (ROI2) or the dual ROI (ROI1 + ROI2) approach. However, CST fiber tracking that was solely based on the anatomical ROI (ROI1) showed significantly compromised integrity because of the mass effect of the lesion on the brain tissue. The validity of our approach can be observed in supplementary Figure S1, http://links.lww.com/MD/A849, which shows all of the CST results for Group I patients (patients 1, 3, 4, 6, 10, and 11).

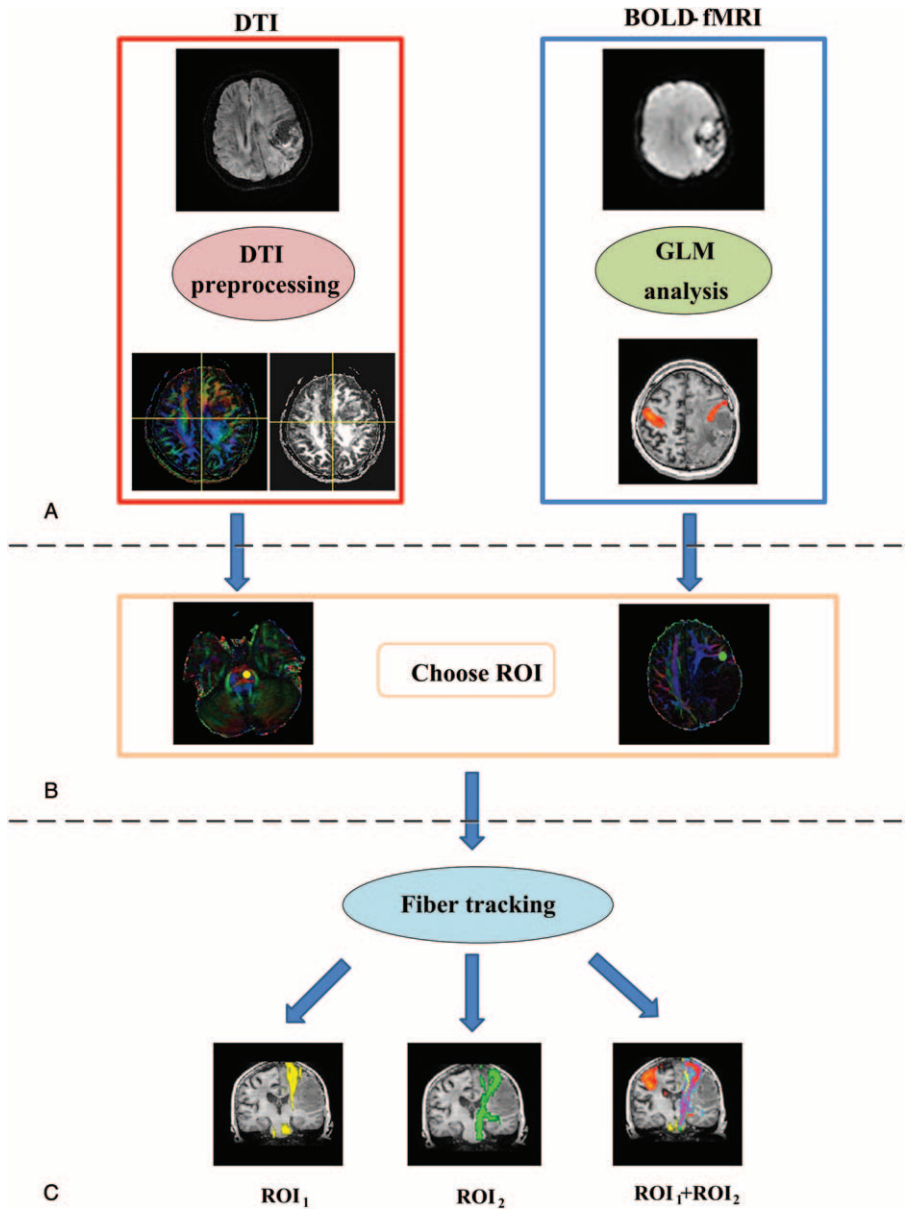

FIGURE 1. A flow chart of the data-processing steps. (A) DTI and task-based fMRI data analysis. (B) Fiber tracking ROI defined by color-coded FA maps and fMRI activation maps. The pons and PMC are labeled. (C) The CST was tracked using different ROI selection schemes.CST = corticospinal tract, DTI = diffusion tensor imaging, fMRI = functional MRI, FA = fractional anisotropy, PMC = primary motor cortex, ROI = region-of-interest.

Patients With a Tumor in the PMC That Affected the Internal Capsule

Group II patients (patients 7, 12, 13, 15 and 16) had a lesion in the PMC that affected the internal capsule. In these patients, the PMC and the internal capsule showed different degrees of deformation depending on the tumor mass effect. Figure 3 shows the CST fiber tracking results for patient 12. Patient 12 had a confirmed pathological diagnosis of grade II oligodendroglioma in the left parietal-occipital lobe. In this case, the lesion was located in the left M1 cortex and affected the left internal capsule. Figure 3A shows the lesion and the motor-activated area displayed on a T1-weighted image. Figure 3B and Figure 3C show the CST fiber tracking results based on different ROIs; yellow, green, and purple represent the CST fiber tracking results obtained by using ROI_1, ROI_2, and $ROI_1 + ROI_2$, respectively. Supplementary Figure S2, http://links.lww.com/MD/A849 shows all of the CST results for Group II patients (patients 7, 12, 13, 15, and 16), all of whom had a tumor in the PMC that affected the internal capsule.

Patients With a Tumor Distal to the PMC and the Internal Capsule

Group III patients (patients 2, 5, 8, 9, 14) had lesions that were not in the PMC or the internal capsule. Figure 4 shows the

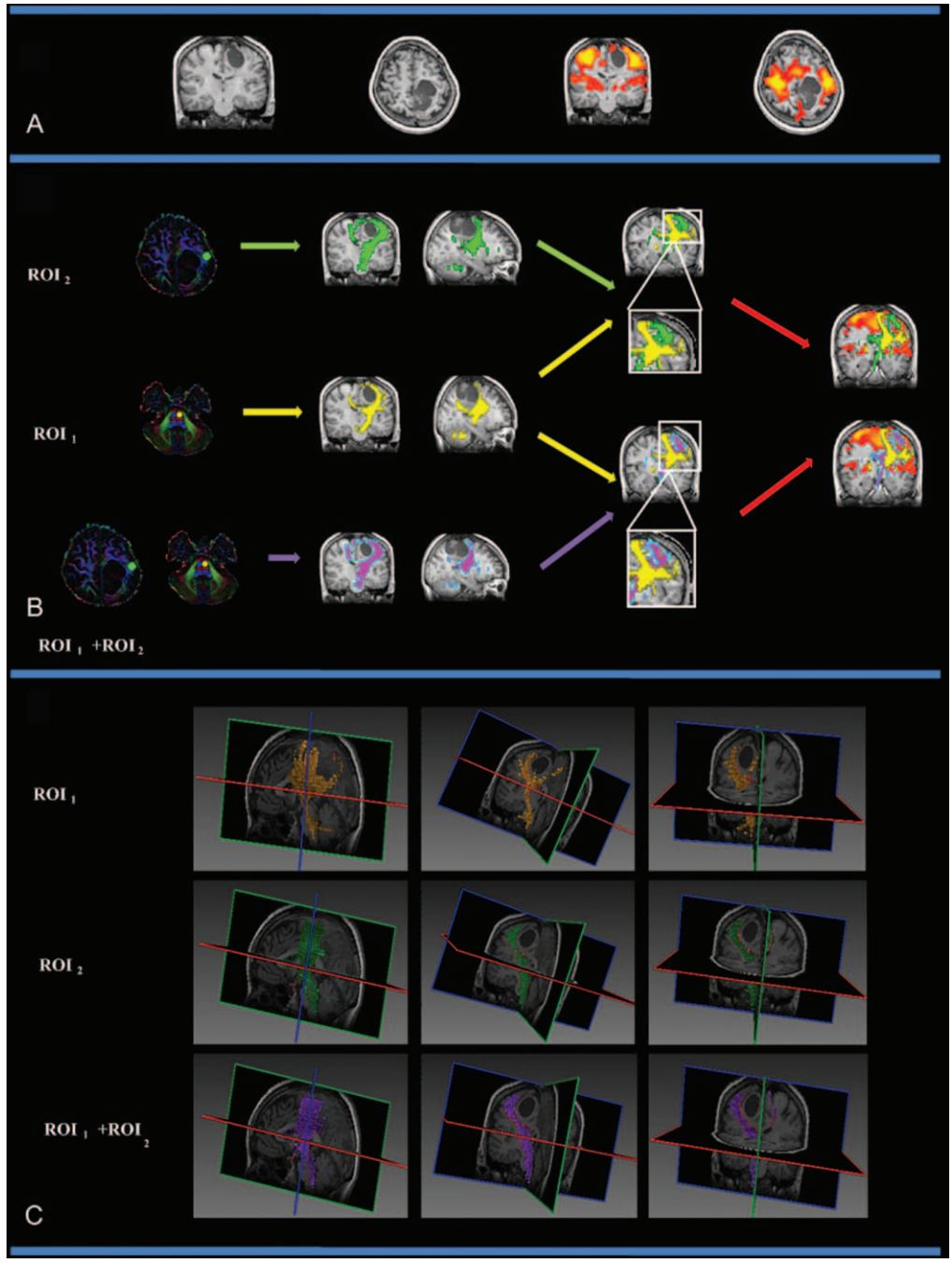

FIGURE 2. The CST fiber tracking results for patient 1. (A) The lesion and motor-activated area are displayed on a T1-weighted image. (B) The CST fiber tracking results based on different ROI definitions. Yellow, green, and purple represent the CST fiber tracking results obtained using ROI1, ROI_2, and $ROI_1 + ROI_2$, respectively. The lesion is located in the left motor area, and it did not affect the left internal capsule. Fiber tracking approaches based on ROI_2 and $ROI_1 + ROI_2$ reached the motor cortex, whereas the reliability of CST tracking solely based on the ROI1 approach was lower due to the tumor mass effect. (C) The 3D visualization of the CST fiber tracking results based on different ROI definitions. CST = corticospinal tract, ROI = region-of-interest.

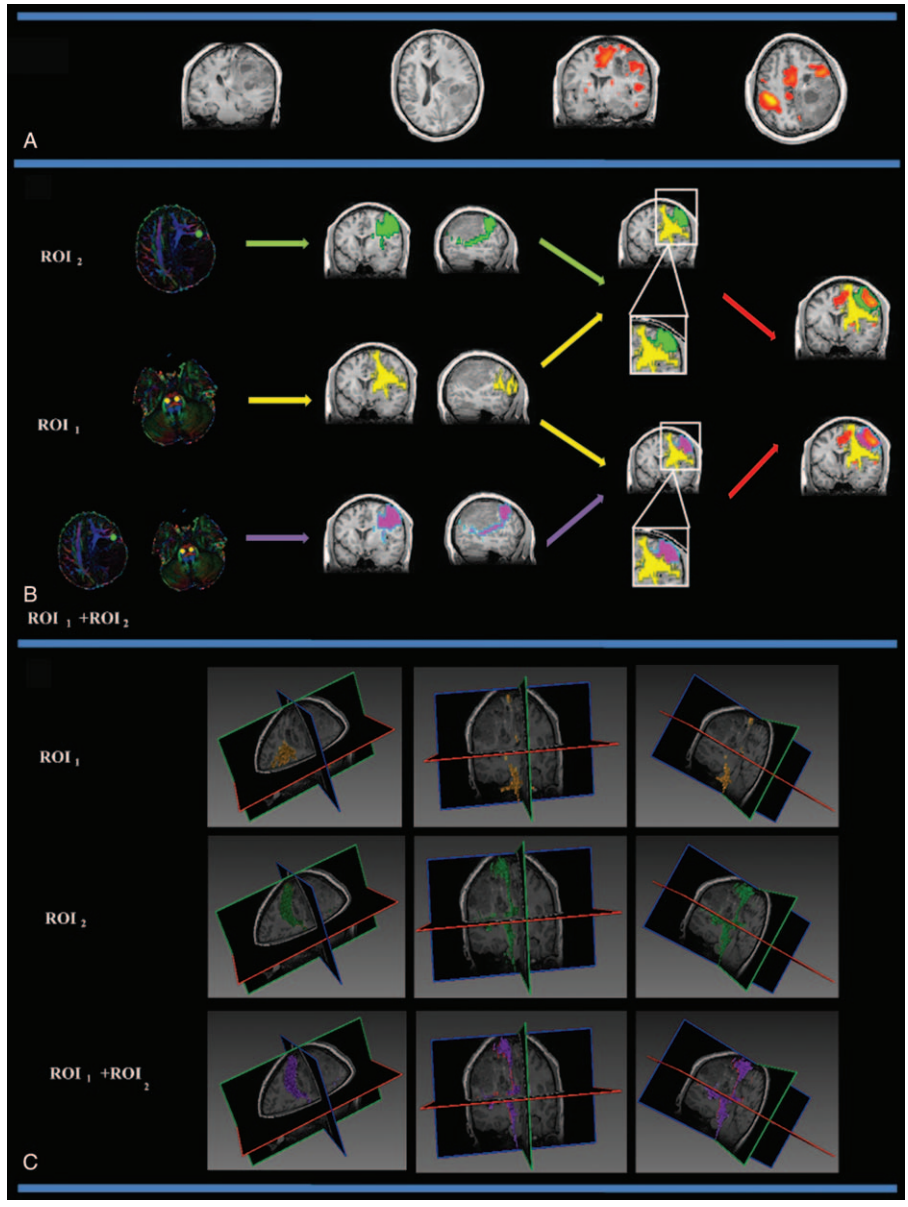

FIGURE 3. The CST fiber tracking results for patient 12, who was diagnosed with a grade II astrocytoma in the left frontal lobe, which affected the motor cortex and the left internal capsule. (A) The lesion and motor-activated area displayed on a T1-weighted image. (B) The CST fiber tracking results based on different ROI definitions. Yellow, green, and purple represent the CST fiber tracking results obtained using ROI_1, ROI_2, and $ROI_1 + ROI_2$, respectively. The CST fiber tracking results based on an anatomical landmark were distorted near the PMC area. When using the fMRI activation area as a seed region, CST fiber tracking reliably reached the motor cortex, and the spatial relationship between the CST and the tumor can be clearly observed. (C) The 3D visualization of the CST fiber tracking results based on different ROI definitions. CST = corticospinal tract, fMRI = functional MRI, PMC = primary motor cortex, ROI = region-of-interest.

CST fiber tracking results for patient 2. Patient 2 had a confirmed pathological diagnosis of transitional meningioma. In this case, the lesion was located in the right frontoparietal lobe and did not affect the motor cortex or the right internal capsule. Figure 4A shows the lesion and the motor activated area on a T1-weighted image. Figure 4B and Figure 4C show the CST fiber tracking results based on different ROIs; yellow, green, and purple represent the CST fiber tracking results obtained using ROI_1, ROI_2, and $ROI_1 + ROI_2$, respectively. Supplementary Figure S3, http://links.lww.com/MD/A849 shows all of the CST results for Group III patients (patients 2, 5, 8, 9, 14), all of whom had a tumor that was distal to the PMC and the internal capsule.

DISCUSSION

The results of our study indicate that the anatomical ROI-based approach for tracking CST fibers is not sufficient for accurately mapping the CST of patients with mass lesions. In contrast, the dual ROI method, which uses ROIs selected from

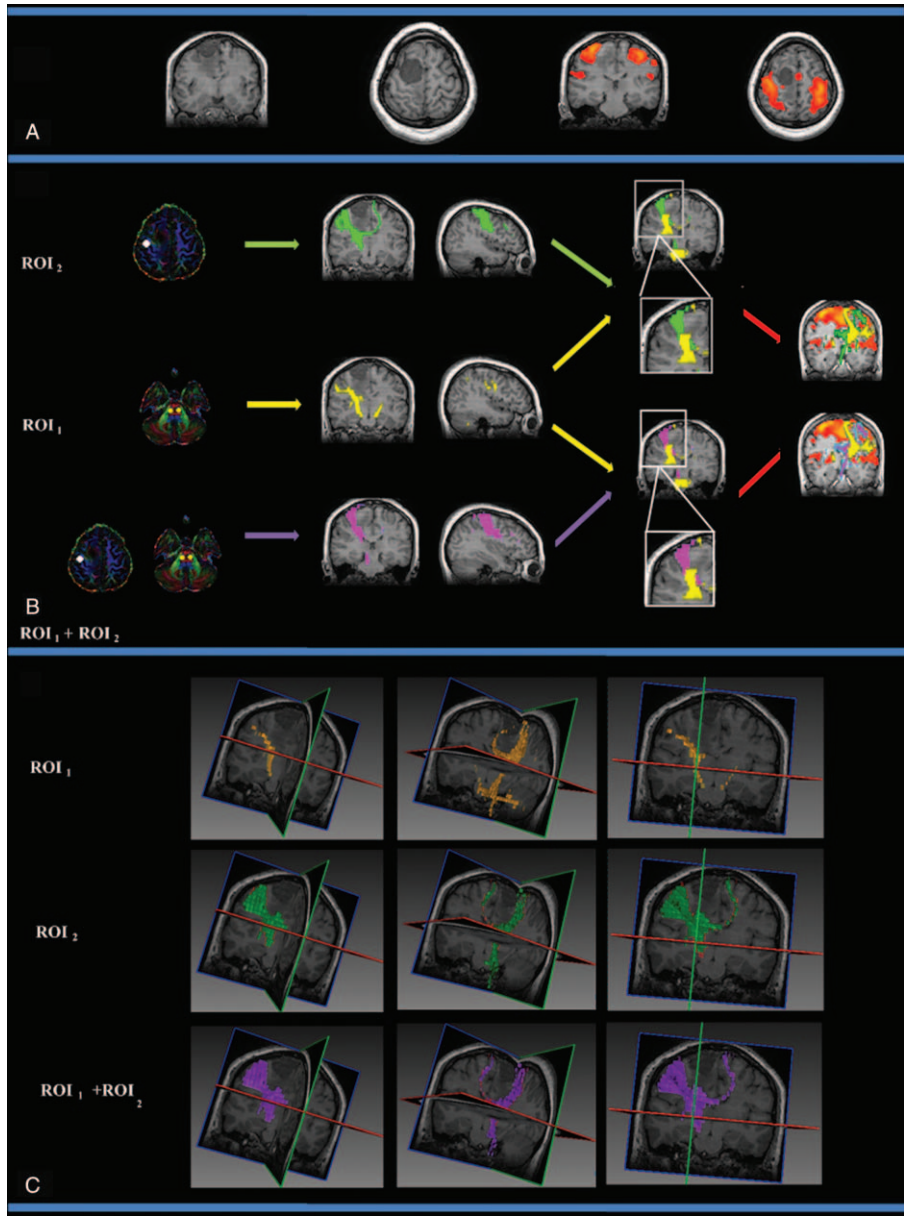

FIGURE 4. The CST fiber tracking results for patient 2, who was diagnosed with transitional meningioma in the right frontal cortex that did not affect the primary motor cortex or the right internal capsule. (A) The lesion and motor-activated area are displayed on a T1-weighted image. (B) The CST fiber tracking results based on different ROI definitions. Yellow, green, and purple represent the CST fiber tracking results obtained using ROI_1, ROI_2, and $ROI_1 + ROI_2$, respectively. fMRI activation is observed in the primary and supplementary motor cortex. Similar fiber tracking results are presented for the fMRI-guided DT approach (ROI_2) and the dual ROI approach ($ROI_1 + ROI_2$). (C) The 3D visualization of the CST fiber tracking results based on different ROI definitions. CST = corticospinal tract, fMRI = functional MRI, ROI = region-of-interest.

fMRI activation and anatomical landmarks, allowed for the CST fiber pathway controlling hand movement to be tracked to the cortex. Our approach identified the entire fiber pathway of the CST as well as the spatial relationship between the CST and the lesions. Furthermore, we found that a dual ROI approach for CST fiber tracking achieved the best results. Taken together, our results illustrate the reliability of fMRI-guided DTI fiber tracking in patients with tumors. The combined functional and anatomical fMRI data enhanced the performance of CST fiber tracking in brains with anatomical deformations or mass lesions. Our approach could be used to provide neurosurgeons with a more accurate method for visualizing and localizing CST white matter pathways during preoperative planning.

Conventional CST fiber tracking is mainly performed using anatomical landmarks (ie, the posterior limb of the internal capsule and/or the anterior pons) to define the fiber tracking ROI.[38–40] Although anatomical ROI mapping is considered a relatively reliable method in healthy subjects,[28] in patients with a brain tumor, the CST white matter fibers may be displaced because of the brain mass lesion. In such cases,

conventional CST fiber tracking using only anatomical ROIs does not allow for accurate tractography.[41,42] In our study, most patients had tumor lesions localized in the motor cortex, and therefore, it was difficult to accurately define anatomically based ROIs in the motor cortex. Therefore, we divided our patients into 3 subgroups based on the spatial relationships between the lesion and the PMC/internal capsule to evaluate CST tracking based on different ROI definitions. We predicted that mass effects would have less of an influence on the CST tractography of patients with brain tumors distal to the PMC. Our results in all 3 subgroups indicated that the dual ROI approach or the fMRI-based ROI generated the most accurate results. Visual checking of the CST fiber tracking results indicates that we could successfully track fibers related to hand movement when using the fMRI-based ROI or the dual ROI approach. Our results indicate that combining BOLD-fMRI with DTI is useful for CST fiber tracking in presurgical clinical applications. In some clinical cases, the fibers displaced by the lesion are adjacent to it. In other cases, the fibers pass within the lesion or could not be specifically identified. Placement of the ROI within the vicinity of a lesion based solely on anatomical landmarks could be subjective and potentially lead to a miscalculation of the fiber pathway. Here, our anatomical ROI was placed in the region of the pons, and very few patients have lesions at this region. Previous studies have suggested that fiber tracking of the CST relative to the pons could provide more information about the characteristics of the white matter.[43] Our results show that BOLD-fMRI activation of the ROI as a seed region and the pons as a target region can provide accurate hand motor-control-related CST fiber tracking. Most previous studies have used the same analytical strategy.[44] Previous studies have reported that using fMRI activation data improve the accuracy of CST fiber tracking. However, in some cases of deep subcortical tumors, the normal position of the PMA may be preserved, whereas only the fiber bundles of the CST may be displaced.[41,45] In such cases, the PMA can no longer be used as a landmark for CST tractography; mass lesions alter both the normal hemodynamic response and the neurovascular coupling. This could result in distorted fMRI activation and should be considered in patients with tumors.[30] In addition, patients with tumors may not be cooperative during fMRI scanning, leading to inaccurate activation results. Furthermore, an approach combining an anatomical ROI and an ROI defined by functional activation can be used to accurately delineate fiber bundles.[46,47]

Over the past few years, accumulating evidence from tractography-guided brain tumor surgery studies reports good clinical outcomes.[48] In particular, the recent studies showed that the combination of the intraoperative subcortical stimulation and DTI fiber tracking would further prove the benefit of tractography-guided neurosurgery planning.[49–51] However, to date, choosing subcortical ROIs remains a controversial process. The posterior limb of the internal capsule and/or the anterior pons are the most often used subcortical ROIs for CST fiber tracking.[33,52] Weiss et al[46] suggested that the use of an ROI at the anterior pontine level (aiP) leads to more reliable and plausible tractography results compared to the use of a subcortical ROI defined by the posterior limb of the internal capsule (PLIC). Furthermore, combining multiple ROIs (aiP, PLIC) for CST fiber tracking does not significantly improve CST tracking performance. However, it may be helpful in particular cases.[46] In our study, mass lesions distorted the internal capsule in several patients, so we could not reliably use the internal capsule as an anatomical landmark for CST fiber tracking; thus, we choose the pons region.

This study has several limitations. First, only 16 patients were included, and such a small sample size reduces the confidence in our findings. However, despite the small sample size, our results clearly demonstrate the advantage of a dual ROI approach in reliably reconstructing white matter tracts that extend to the cortex. Such precise reconstruction is not possible using only anatomical methods, and our results provide critical guidance for future neurosurgical practices. The second limitation of our study is that only a handgrip task was used for the fMRI session. Previous studies have suggested that subcomponents of the CST are better differentiated using different tasks. Previous studies have reported an incomplete CST tractography when placing the ROI in the medulla oblongata (eg, the fibers connecting to the lip could not be reconstructed).[45,48] In the present study, we chose to use the pons as an anatomical landmark because the internal capsule was distorted by the brain tumor. In future studies, we will increase the sample size and perform multiple stimulation tasks to differentiate subcomponents of the CST. We will also increase the tumor-location subgroups and tumor-pathology subgroups to further evaluate the validity of our approach. The third limitation of the present study is that we used linear registration for the T1, DTI, and BOLD-fMRI datasets. Previous studies have demonstrated that linear registration can provide precise registration for applications within individual subject's brain tumors.[53,54] Our study also demonstrated that the linear registration method is useful for routine clinical MRI applications involving brain tumors. However, by utilizing more sophisticated algorithms, the registration accuracy, and thus the reproducibility of tractography results, could be improved. In the future, we will further evaluate the different registration approaches for preneurosurgical applications and determine the best strategy for routine clinical use.[55]

CONCLUSIONS

In conclusion, we evaluated a combinatorial approach that used functional activation and anatomical landmark data to define multiple ROIs for CST fiber tracking in patients with brain tumors. Our results suggest that a combination of BOLD-fMRI and DTI fiber tracking may provide a more comprehensive analysis of the CST pathway, which would be beneficial for characterizing the spatial relationships between the CST pathway and the tumor. A dual ROI CST fiber tracking approach has the potential to play a critical role in preoperative planning to optimize surgical treatment and in improving postsurgical outcomes.

ACKNOWLEDGMENTS

This study was supported by the National Natural Science Foundation of China (Project No. 61473221, 81171318, 61401363, 81571640 and 61262034), by Doctoral Fund of Ministry of Education of China (20120201120071), by Nature Science Foundation of Shaan Xi Province of China (2015JM3105) and by the Fundamental Research Funds for the Southeast Universities of China (CDLS-2015–05).

REFERENCES

1. Chaichana KL, Halthore AN, Parker SL, et al. Factors involved in maintaining prolonged functional independence following supratentorial glioblastoma resection. Clinical article. *J Neurosurg.* 2011;114:604–612.

2. Sanai N, Berger MS. Glioma extent of resection and its impact on patient outcome. *Neurosurgery.* 2008;62:753–764discussion 264-6.
3. Duffau H. Lessons from brain mapping in surgery for low-grade glioma: insights into associations between tumour and brain plasticity. *Lancet Neurol.* 2005;4:476–486.
4. Iwasaki S, Nakagawa H, Fukusumi A, et al. Identification of pre- and postcentral gyri on CT and MR images on the basis of the medullary pattern of cerebral white matter. *Radiology.* 1991;179:207–213.
5. Berger MS. Minimalism through intraoperative functional mapping. *Clin Neurosurg.* 1996;43:324–337.
6. Duffau H, Capelle L, Sichez N, et al. Intraoperative mapping of the subcortical language pathways using direct stimulations. *Brain.* 2002;125:199–214.
7. Gaetz W, Scantlebury N, Widjaja E, et al. Mapping of the cortical spinal tracts using magnetoencephalography and diffusion tensor tractography in pediatric brain tumor patients. *Childs Nerv Syst.* 2010;26:1639–1645.
8. Stippich C. Presurgical functional MRI and diffusion tensor imaging. In: Stippich C, ed. *Clinical Functional MRI.* Berlin, Heidelberg: Springer; 2015:1–12.
9. Tozakidou M, Wenz H, Reinhardt J, et al. Primary motor cortex activation and lateralization in patients with tumors of the central region. *Neuroimage Clin.* 2013;2:221–228.
10. Sugishita M. [Clinical application of functional magnetic resonance imaging]. *No To Hattatsu.* 2002;34:111–118.
11. Stippich C, Blatow M, Garcia M. Task-based presurgical functional MRI in patients with brain tumors. In: Stippich C, ed. *Clinical Functional MRI.* Berlin, Heidelberg: Springer; 2015:89–141.
12. Kapsalakis IZ, Kapsalaki EZ, Gotsis ED, et al. Preoperative evaluation with FMRI of patients with intracranial gliomas. *Radiol Res Pract.* 2012;2012:1–17.
13. Schulder M, Maldjian JA, Liu WC, et al. Functional image-guided surgery of intracranial tumors located in or near the sensorimotor cortex. *J Neurosurg.* 1998;89:412–418.
14. Niu C, Zhang M, Min Z, et al. Motor network plasticity and low-frequency oscillations abnormalities in patients with brain gliomas: a functional MRI study. *PLoS One.* 2014;9:e96850.
15. Cho HM, Choi BY, Chang CH, et al. The clinical characteristics of motor function in chronic hemiparetic stroke patients with complete corticospinal tract injury. *NeuroRehabilitation.* 2012;31:207–213.
16. Jang SH. The corticospinal tract from the viewpoint of brain rehabilitation. *J of Rehabil Med.* 2014;46:193–199.
17. Laundre BJ, Jellison BJ, Badie B, et al. Diffusion tensor imaging of the corticospinal tract before and after mass resection as correlated with clinical motor findings: preliminary data. *AJNR Am J Neuroradiol.* 2005;26:791–796.
18. Le Bihan D, Mangin JF, Poupon C, et al. Diffusion tensor imaging: concepts and applications. *J Magn Reson Imag.* 2001;13:534–546.
19. Pierpaoli C, Jezzard P, Basser PJ, et al. Diffusion tensor MR imaging of the human brain. *Radiology.* 1996;201:637–648.
20. Mori S, van Zijl PC. Fiber tracking: principles and strategies - a technical review. *NMR Biomed.* 2002;15:468–480.
21. Yamada K, Mori S, Nakamura H, et al. Fiber-tracking method reveals sensorimotor pathway involvement in stroke patients. *Stroke.* 2003;34:E159–E162.
22. Berman JI, Berger MS, Chung SW, et al. Henry Accuracy of diffusion tensor magnetic resonance imaging tractography assessed using intraoperative subcortical stimulation mapping and magnetic source imaging. *J Neurosurg.* 2007;107:488–494.
23. Berman JI, Berger MS, Mukherjee P, et al. Diffusion-tensor imaging-ided tracking of fibers of the pyramidal tract combined with intraoperative cortical stimulation mapping in patients with gliomas. *J Neurosurg.* 2004;101:66–72.
24. Nilsson D, Rutka JT, Snead OC 3rd et al. Preserved structural integrity of white matter adjacent to low-grade tumors. *Childs Nerv Syst.* 2008;24:313–320.
25. Kleiser R, Staempfli P, Valavanis A, et al. Impact of fMRI-guided advanced DTI fiber tracking techniques on their clinical applications in patients with brain tumors. *Neuroradiology.* 2010;52:37–46.
26. Wieshmann UC, Symms MR, Parker GJ, et al. Diffusion tensor imaging demonstrates deviation of fibres in normal appearing white matter adjacent to a brain tumour. *J Neurol Neurosurg Psychiatry.* 2000;68:501–503.
27. Witwer BP, Moftakhar R, Hasan KM, et al. Diffusion-tensor imaging of white matter tracts in patients with cerebral neoplasm. *J Neurosurg.* 2002;97:568–575.
28. Schonberg T, Pianka P, Hendler T, et al. Characterization of displaced white matter by brain tumors using combined DTI and fMRI. *Neuroimage.* 2006;30:1100–1111.
29. Lehericy S, Duffau H, Cornu P, et al. Correspondence between functional magnetic resonance imaging somatotopy and individual brain anatomy of the central region: comparison with intraoperative stimulation in patients with brain tumors. *J Neurosurg.* 2000;92:589–598.
30. Wehner T. The role of functional imaging in the tumor patient. *Epilepsia.* 2013;54(Suppl 9):44–49.
31. Zaca D, Jovicich J, Nadar SR, et al. Cerebrovascular reactivity mapping in patients with low grade gliomas undergoing presurgical sensorimotor mapping with BOLD fMRI. *J Magn Reson Imaging.* 2014;40:383–390.
32. Goebell E, Paustenbach S, Vaeterlein O, et al. Low-grade and anaplastic gliomas: differences in architecture evaluated with diffusion-tensor MR imaging. *Radiology.* 2006;239:217–222.
33. Mandelli ML, Berger MS, Bucci M, et al. Quantifying accuracy and precision of diffusion MR tractography of the corticospinal tract in brain tumors. *J Neurosurg.* 2014;121:349–358.
34. Louis DN, Ohgaki H, Wiestler OD, et al. The 2007 WHO classification of tumours of the central nervous system. *Acta neuropathologica.* 2007;114:97–109.
35. Jenkinson M, Beckmann CF, Behrens TE, et al. FSL. *Neuroimage.* 2012;62:782–790.
36. Smith SM, Jenkinson M, Johansen-Berg H, et al. Tract-based spatial statistics: voxelwise analysis of multi-subject diffusion data. *Neuroimage.* 2006;31:1487–1505.
37. Woolrich MW, Jbabdi S, Patenaude B, et al. Bayesian analysis of neuroimaging data in FSL. *Neuroimage.* 2009;45((1 Suppl)):S173–S186.
38. Akai H, Mori H, Aoki S, et al. Diffusion tensor tractography of gliomatosis cerebri: fiber tracking through the tumor. *J Comput Assist Tomogr.* 2005;29:127–129.
39. Catani M, Howard RJ, Pajevic S, et al. Virtual in vivo interactive dissection of white matter fasciculi in the human brain. *NeuroImage.* 2002;17:77–94.
40. Holodny AI, Gor DM, Watts R, et al. Diffusion-tensor MR tractography of somatotopic organization of corticospinal tracts in the internal capsule: initial anatomic results in contradistinction to prior reports. *Radiology.* 2005;234:649–653.
41. Mori S, Frederiksen K, van Zijl PC, et al. Brain white matter anatomy of tumor patients evaluated with diffusion tensor imaging. *Ann Neurol.* 2002;51:377–380.

42. Wei CW, Guo G, Mikulis DJ. Tumor effects on cerebral white matter as characterized by diffusion tensor tractography. *Can J Neurol Sci.* 2007;34:62–68.

43. Seo JP, Jang SH. Characteristics of corticospinal tract area according to pontine level. *Yonsei Med J.* 2013;54:785–787.

44. Kumar A, Juhasz C, Asano E, et al. Diffusion tensor imaging study of the cortical origin and course of the corticospinal tract in healthy children. *AJNR Am J Neuroradiol.* 2009;30:1963–1970.

45. Ebeling U, Reulen HJ. Subcortical topography and proportions of the pyramidal tract. *Acta Neurochirurgica.* 1992;118:164–171.

46. Weiss C, Tursunova I, Neuschmelting V, et al. Improved nTMS- and DTI-derived CST tractography through anatomical ROI seeding on anterior pontine level compared to internal capsule. *Neuroimage Clin.* 2015;7:424–437.

47. Radmanesh A, Zamani AA, Whalen S, et al. Comparison of seeding methods for visualization of the corticospinal tracts using single tensor tractography. *Clin Neurol Neurosurg.* 2015;129:44–49.

48. Wu JS, Zhou LF, Tang WJ, et al. Clinical evaluation and follow-up outcome of diffusion tensor imaging-based functional neuronavigation: a prospective, controlled study in patients with gliomas involving pyramidal tracts. *Neurosurgery.* 2007;61:935–948discussion 48-9.

49. Bucci M, Mandelli ML, Berman JI, et al. Quantifying diffusion MRI tractography of the corticospinal tract in brain tumors with deterministic and probabilistic methods. *Neuroimage Clin.* 2013;3:361–368.

50. Frey D, Strack V, Wiener E, et al. A new approach for corticospinal tract reconstruction based on navigated transcranial stimulation and standardized fractional anisotropy values. *Neuroimage.* 2012;62:1600–1609.

51. Ohue S, Kohno S, Inoue A, et al. Accuracy of diffusion tensor magnetic resonance imaging-based tractography for surgery of gliomas near the pyramidal tract: a significant correlation between subcortical electrical stimulation and postoperative tractography. *Neurosurgery.* 2012;70:283–293discussion 94.

52. D'Andrea G, Angelini A, Romano A, et al. Intraoperative DTI and brain mapping for surgery of neoplasm of the motor cortex and the corticospinal tract: our protocol and series in BrainSUITE. *Neurosurg Rev.* 2012;35:401–412discussion 12.

53. Bailey PD, Zaca D, Basha MM, et al. Presurgical fMRI and DTI for the prediction of perioperative motor and language deficits in primary or metastatic brain lesions. *J Neuroimag.* 2015;25:776–784.

54. Campanella M, Ius T, Skrap M, et al. Alterations in fiber pathways reveal brain tumor typology: a diffusion tractography study. *PeerJ.* 2014;2:e497.

55. Liu X, Yang Y, Sun J, et al. Reproducibility of diffusion tensor imaging in normal subjects: an evaluation of different gradient sampling schemes and registration algorithm. *Neuroradiology.* 2014;56:497–510.